

# Circularly polarised equilateral triangular patch antenna for mobile satellite communications

J.T. Sri Sumantyo and K. Ito

**Abstract:** A left-handed circularly polarised (LHCP) triangular patch antenna is developed to support the next generation of mobile satellite communications using Engineering Test Satellite VIII (ETS-VIII). The targeted minimum gain of the antenna is set to 5 dBic for applications of a hundred kbps data transfer with an axial ratio less than 3 dB for circular polarisation. A dual-proximity-coupled equilateral triangular patch antenna is proposed and simulated by the method of moments (MoM) for finite and infinite ground plane models to investigate the ground plane effect. Then measurements of the fabricated antenna are performed to confirm the simulation results. The measurement results show that the frequency characteristics of the fabricated antenna is 0.2% shifted to the higher frequency, and the maximum gain is 0.45 dB lower than the result of the finite ground plane model. Additionally, the simulation results show the ground plane size influences the antenna characteristics, especially the gain and axial ratio of the developed antenna.

## 1 Introduction

The Japan Aerospace Exploration Agency (JAXA) will launch a geostationary satellite called Engineering Test Satellite VIII (ETS-VIII) in 2006. ETS-VIII will conduct orbital experiments on mobile satellite communications at the S-band frequency, especially to support the development of a technology for the transmission and reception of multimedia information, such as voice and images for land mobile systems [1]. Up to now, various antennas have been developed for mobile satellite communications purposes [2, 3], but these antennas have a complex composition. Therefore, in this research, a simple satellite-tracking triangular patch antenna is proposed to solve this problem. The targeted minimum gain of the antenna is set to 5 dBic for applications of a hundred kbit/s data transfer. The antenna should also be designed as thin, compact and as small and simple as possible, because it will be mounted on an aircraft, a small boat or a car roof [4].

The result obtained in this research, in the near future, would also be assessed for hand-held antenna and a simple satellite-tracking triangular patch array antenna for ETS-VIII or mobile satellite communications applications. Especially, the configuration of the triangular patch array antenna, by using the developed antenna as shown in Fig. 1, is proposed as an improvement on previous antennas [5, 6], where the beam of the antenna to track the satellite is generated by a simple mechanism that consists in switching off one of the radiating element of reception (Rx) or transmission (Tx). By considering the mutual coupling between fed elements, their phase and distance, the beam

direction can be varied. Hence, the two fed elements theoretically generate a beam shift of  $-90^\circ$  in the conical-cut direction from the element which is turned off, in the case of a left-handed circular polarisation (LHCP) antenna and a single band with only three elements. For example, as shown in Fig. 2, when Element 1 of reception (Rx1) is off, the beam is theoretically directed towards the azimuth angle  $Az=0^\circ$ . In the same manner, the other two beams of reception can be generated by successively switching off each element (Rx2 and Rx3 in Fig. 1) and the beam will be directed towards  $Az=120^\circ$  and  $Az=240^\circ$ . Then the three beams of transmission (Tx) can also be switched in the same way.

## 2 Specifications and targets

Table 1 shows the specifications and targets of the antenna for mobile satellite communications aiming at ETS-VIII

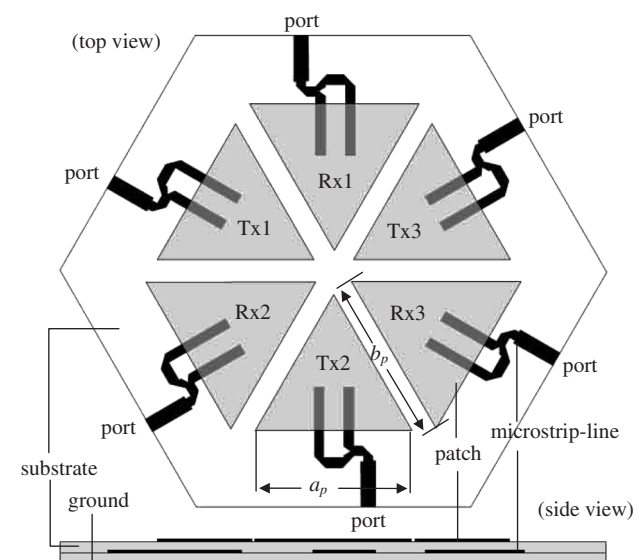


Fig. 1 Configuration of dual-band triangular patch array antenna

© The Institution of Engineering and Technology 2006

IEE Proceedings online no. 20045129

doi:10.1049/ip-map:20045129

Paper first received 7th October 2004 and in final revised form 24th October 2005

J.T. Sri Sumantyo is with the Centre for Environmental Remote Sensing, Chiba University, 1-33, Yayoi, Inage, Chiba, 263-8522 Japan

K. Ito is with the Graduate School of Science and Technology, Chiba University, 1-33, Yayoi, Inage, Chiba, 263-8522 Japan

E-mail: tetuko@restaff.chiba-u.jp

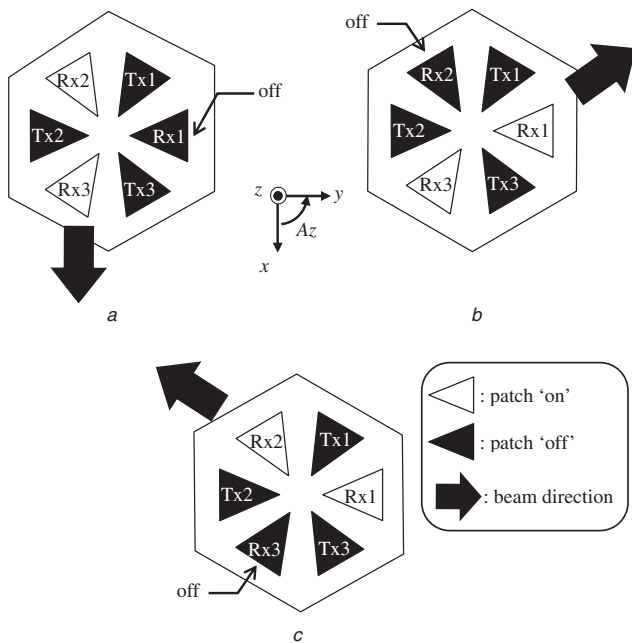


**Fig. 2** Switching mechanism of developed antenna

- a Rx1 patch off
- b Rx2 patch off
- c Rx3 patch off

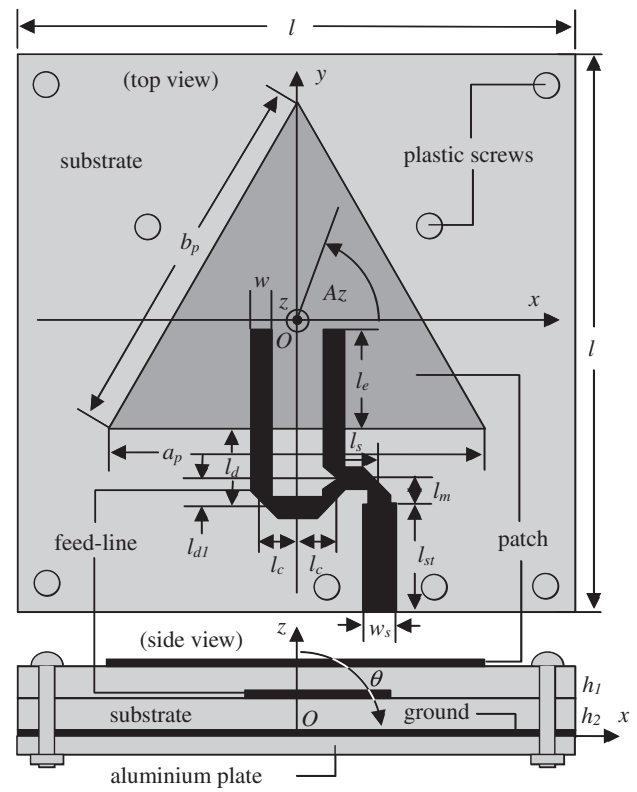


**Fig. 3** Configuration of the developed triangular patch antenna

**Table 1: Specifications and targets of the antenna for ETS-VIII applications**

Specifications		
Frequency bands	Transmission (Tx)	2655.5–2658.0 MHz
	Reception (Rx)	2500.5–2503.0 MHz
Polarisation	Left-handed circular polarisation for both transmission and reception	
Targets		
Minimum gain	5 dBic	
Maximum axial ratio	3 dB	

applications that are used in this research, especially the patch antenna for reception (Rx) only. However, the transmission (Tx) can be designed similarly. Here, a thin miniaturised antenna designed for a hundred kbit/s data transfer (minimum gain 5 dBic) is simulated. In this research, a dual-proximity-coupled equilateral triangular patch antenna for reception is investigated. The operating frequency is fixed at 2.5025 GHz. In addition, the targeted axial ratio is less than 3 dB in order to obtain good circular polarisation. Then the comparison of finite and infinite ground planes of the patch antenna is simulated to investigate the effect of ground plane size on the characteristics of the antenna.

### 3 Configuration of the equilateral triangular patch

Figure 3 shows the configuration of a developed triangular patch antenna. In order to satisfy the specifications of ETS-VIII, the antenna is designed and fabricated using a conventional substrate (relative permittivity  $\epsilon_r = 2.17$  and

$\tan \delta = 0.00085$ ), where the substrate thicknesses for triangular patch ( $h_1$ ) and microstripline ( $h_2$ ) are both 0.8 mm. Thus, the total thickness of this antenna is 1.6 mm. Then the conductor of the triangular patch, microstripline feed and ground employed is a perfect conductor ( $\tan \delta = 0$ ). The length of substrate and ground plane is set to 81.5 mm as shown in Fig. 3. This configuration is used for the sake of compactness, and most importantly to obtain a satisfactory gain and axial ratio.

Several types of circularly polarised triangular antennas were previously developed [5], but they are difficult to design and optimise because the ratio between  $a_p$  and  $b_p$  (see Fig. 3) sensitively affects the performance of the axial ratio. Then, the pin feed technique is commonly applied to generate a circular polarisation for the triangular antenna, but this technique is more complex than the microstripline or proximity feed technique in the fabrication process. Basically, this pin feed technique with a single feed point will generate an unstable current distribution on each patch when the patches are composed in array configuration [6, 7]. Thus, we propose here a feeding technique using a microstripline, as shown in Fig. 3, for equilateral triangular patches because this configuration is easier to design and fabricate without any optimisation of the ratio between  $a_p$  and  $b_p$ . With such a technique, a stable current distribution can be obtained on the triangular patch surface, thus generating a circular polarisation. Hence, it can improve the performance of the previously developed antennas [6, 7] and a compact and small configuration can be obtained.

The triangular patch is fed by proximity coupling with a microstripline whose width  $w$  is 3.0 mm. The dual-feed type is proposed to generate a left-handed circular polarisation (LHCP), where one branch of the microstripline is  $\lambda/4$  longer than the other one to induce a  $90^\circ$  phase delay. The detailed parameters of the microstripline are  $l_e = 14$  mm,  $l_s = 5$  mm,  $l_d = 11$  mm,  $l_{d1} = 4$  mm,  $l_c = 5$  mm,  $l_m = 2$  mm,  $l_{st} = 11$  mm and  $w_s = 4.7$  mm.

In this research, the method of moments (MoM) of IE3D (Zeland Software Inc.) and Ensemble™ Ver.8 (Ansoft) were employed to simulate the models with finite and infinite ground planes, respectively. The size of the finite substrate and ground plane in the simulation model matches the fabricated antenna ( $l = 81.5$  mm). The length of the microstripline inserted under the patch ( $l_c$ ) is 14 mm, and a quarter-wave transformer with a length  $l_{st} = 11$  mm is used to obtain a matching impedance of  $50 \Omega$ . Then, the microstripline is fed by an SMA connector on the edge of the substrate. The fabricated triangular patch antenna is shown in Fig. 4. The patch length  $a_p$  is optimised to find the patch width of the fabricated antenna resonating at  $f = 2.5025$  GHz and the size of the patch ( $a_p = b_p$ ) obtained is 52.8 mm.

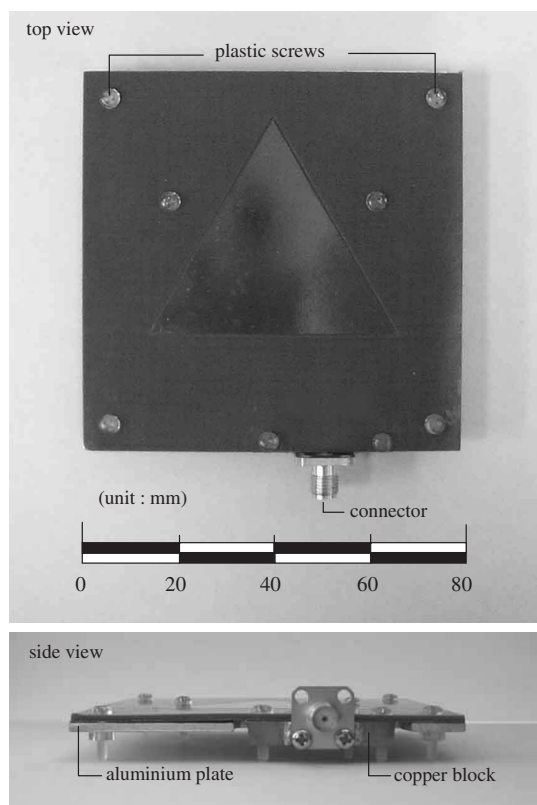


Fig. 4 Fabricated triangular patch antenna

As shown in Figs. 3 and 4, plastic screws are used to fix the two layers (substrate and aluminium plate) that compose the antenna, to obtain stable measurement results. The aluminium plate (2 mm thick) is used to support the substrate, for it to be always flat, because it is thin and easily foldable.

The measurements of the fabricated antenna were done in the anechoic chamber of the Graduate School of Science and Technology, Chiba University, Japan. The gain of the antenna was measured by using a circularly polarised conical spiral antenna. In the case of the axial ratio measurement, LHCP and RHCP conical spiral antennas were employed. Then the field intensity obtained by measurement was compared with the measurement result of a standard dipole and shown in dBic. In the following Section, the measurement results are used to confirm the simulation results.

#### 4 Measurement results and discussions

Figure 5 shows the relationship between the reflection coefficient ( $S_{11}$ ) and the frequency for the simulation model

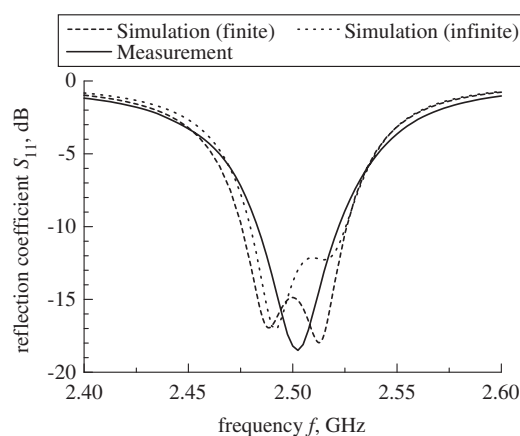


Fig. 5 Reflection coefficient against frequency

(finite and infinite ground planes) and the fabricated antenna. From this figure, the centre frequency of measurement matches well to the simulation models. However, the  $-10$  dB bandwidth of measurement is 0.4% and 0.3% different from the finite and infinite ground plane models, respectively. This bandwidth difference is due to the fabrication error (drilling error about 0.1 mm in manufacturing) and the influence of the measurement system (connector, aluminium plate, copper block to support the connector, holes for plastic screws, etc.). The result also proves that the ground plane size has an effect on the antenna characteristics, especially the reflection coefficient.

The relationship between the input impedance  $Z_{in}$  and frequency of simulation model and measurement is shown in Fig. 6. The same reason as above induces the characteristic of impedance.

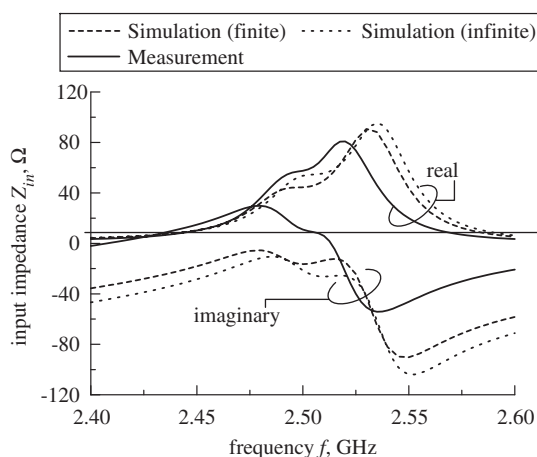


Fig. 6 Input impedance against frequency

The developed antenna is left-handed circularly polarised. Therefore, the performance is investigated in terms of axial ratio  $Ar$  characteristics as shown in Fig. 7. This figure depicts the relationship between  $Ar$  and the frequency for the simulation model as well as the measurement results for a theta angle  $\theta = 0^\circ$  or in the direction to the center  $O$  (see Fig. 3). This figure shows that the frequency characteristics of the measurement ( $f = 2.5025$  GHz) and infinite ground plane model are shifted 0.2% to the higher frequency compared to the finite ground plane model. As a result of this research, it is shown that the fabrication error and the configuration of the fabricated antenna (connector,

aluminium plate, copper block, holes for plastic screws, etc.) also influence the characteristics of a circularly polarised patch array antenna, as can be seen from the axial ratio characteristics, where the antenna characteristics of the simulation model and measurement are considered at each respective frequency of the minimum axial ratio.

Figure 7 also shows the relationship between the gain  $G$  and the frequency. The maximum gain of measurement is similarly shifted 0.2% and 0.1% to the higher frequency compared to the finite and infinite ground plane models, respectively. Then it is 0.45 dB lower compared to the finite ground plane model, and 0.4 dB higher compared to the infinite ground plane model. When the measurement result is compared to that of the finite ground plane model, the reduction of maximum gain is supposed to be due to the effect of loss in the measurement system. However, the losses occurring in the coaxial cable were considered.

Figure 8 shows that the developed antenna has efficiency 83%, 84% and 85% for finite, infinite ground plane models (simulation) and measurement, respectively, at  $f=2.5025$  GHz. The efficiencies of simulation models were calculated by the pattern integral method. Then, the antenna efficiency of measurement was calculated by using the  $Q$  factor method, where the antenna efficiency  $\eta_r$  is defined as below [8, 9].

$$\eta_r = \frac{Q_{RL}}{Q_R} \quad (1)$$

The  $Q_{RL}$  and  $Q_R$  factors are total quality factor and quality factor due to radiation loss, respectively. The  $Q_{RL}$  and  $Q_R$  is

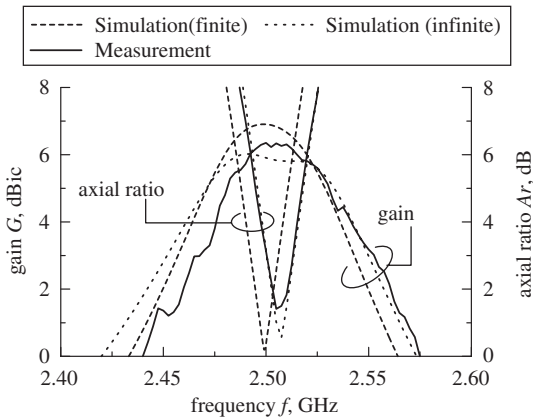


Fig. 7 Gain and axial ratio against frequency at theta angle  $\theta = 0^\circ$

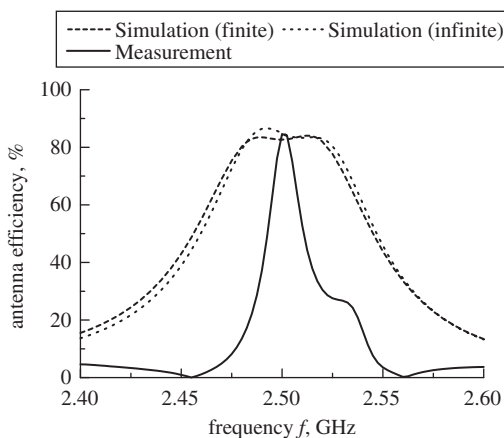


Fig. 8 Efficiency of the developed antenna

acquired by measurement and simulation (it is employed as an ideal or no loss antenna) and are expressed by

$$Q_{RL} = \frac{\omega E_S}{P_R + P_L} \quad (2)$$

$$Q_R = \frac{\omega E_S}{P_R} \quad (3)$$

where  $\omega$  is bandwidth of  $Q$  when the power reflection coefficient is half (or  $-10$  dB in Fig. 5). Then inner power  $E_S = |I|^2 X$  and radiation power  $P_R = |I|^2 R_r$ . The reactance  $X$  and resistance  $R_r$  of simulation and measurement are acquired by input impedance of simulated models and measurement, respectively, as shown in Fig. 6. Then  $P_L$  is loss power that is consumed by the connector, coaxial cable, substrate etc. The measurement result shows a narrow efficiency bandwidth. However, the efficiency at 2.5025 GHz reaches 85%. It is considered by the influence of unmatching input impedance between the measurement and simulation (finite ground plane model as ideal antenna) in the frequency domain as shown in Fig. 6.

Previous reports explained that the finite ground plane induces diffraction effects from the edges of the ground plane resulting in changes in radiation pattern and performance of antenna [10, 11]. This effect also changes the performance of the developed antenna in the theta plane (e.g.  $x-z$  and  $y-z$  planes in Fig. 3) in the case of a circularly polarised patch array antenna, as explained later in detail.

Figures 9 and 10 depict the relationship between  $G$  and  $\theta$  at an azimuth angle  $Az = 0^\circ$  ( $x-z$  plane) and  $90^\circ$  ( $y-z$  plane). First, Fig. 9 shows the relationship between the beam direction and theta angle  $\theta$  in the theta plane at  $Az = 0^\circ$  ( $x-z$  plane). The 5-dBic-gain beamwidth by finite, infinite ground plane models (simulation) and measurement are  $60^\circ$ ,  $63^\circ$  and  $52^\circ$ , respectively. From this figure, the maximum gain of measurement is 0.45 dB lower and 0.7 dB higher than the simulation (finite and infinite ground planes, respectively) obtained by MoM. The low gain of measurement compared to the result of the finite ground plane model is due to the various losses occurring during the measurement. This result shows that the effect of ground plane sizes strongly affects the radiation pattern, especially the  $Ar$  characteristic. The configuration of the antenna and the measurement system, i.e. the coaxial cable, the connector, the hole and the plastic screws in substrates, etc. are also considered to affect the current distribution on the surface of the patches, therefore decreasing the  $Ar$  performance.

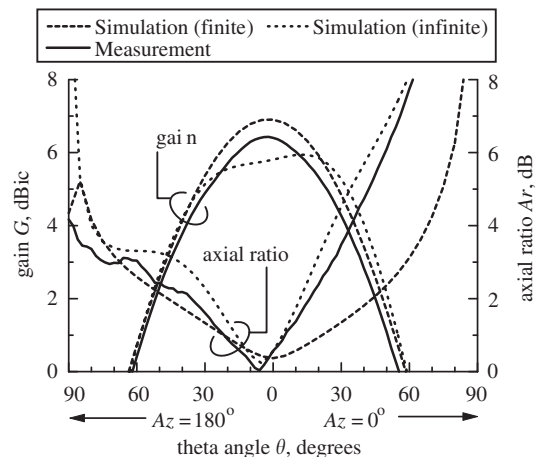
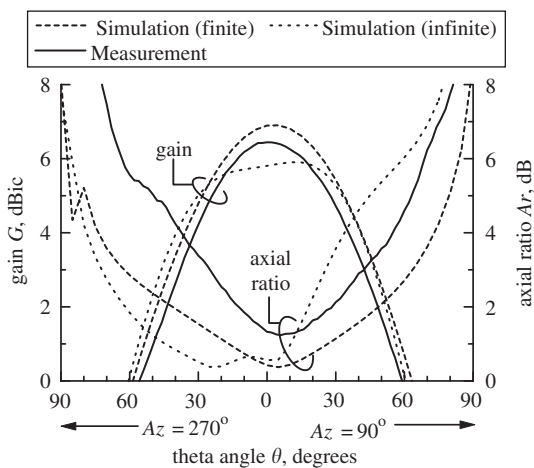


Fig. 9 Radiation pattern in the theta plane ( $Az = 0^\circ$ ) ( $x-z$  plane)



**Fig. 10** Radiation pattern in the theta plane ( $Az = 90^\circ$ ) ( $y$ - $z$  plane)

Finally, Fig. 10 shows the relationship between  $G$ ,  $Ar$  and  $\theta$  at  $Az = 90^\circ$  ( $y$ - $z$  plane). The 5-dBic-gain beamwidth of finite, infinite ground plane models and measurement are  $60^\circ$ ,  $62^\circ$ , and  $52^\circ$ , respectively. From the same figure, the maximum gain of measurement is 0.45 dB lower and 0.7 dB higher than the finite and infinite ground plane models, respectively, obtained by MoM. The same phenomenon as  $Az = 0^\circ$  ( $x$ - $z$  plane) occurs and the same explanation can be applied.

## 5 Conclusions and future developments

JAXA will launch ETS-VIII in 2006 to conduct orbital experiments on mobile satellite communications at the S-band frequency. Therefore, a circularly polarised simple satellite-tracking equilateral triangular patch antenna for mobile satellite communications aiming at ETS-VIII applications was developed in this research. The method of moments (MoM) was employed to design a circularly polarised equilateral triangular patch antenna and to investigate the influence of ground plane size on the performance of the antenna. Then measurements of the fabricated antenna were performed to confirm the simulation results.

The results show that the frequency characteristics of measurement are shifted 0.2% to the higher frequency compared to the finite ground plane model (simulation). This increasing in frequency is due to the influence of the antenna configuration used for the simulation model and the fabricated antenna. The results also show that the frequency characteristics of the axial ratio are sensitively influenced by the ground plane size. The reduction of maximum gain is due to the configuration of the antenna, i.e. the losses occurring in the coaxial cable, connector, copper block, aluminium, hole for plastic screw, etc., and

the effect of ground plane size as infinite ground plane size. The finite ground plane induces diffraction from the edges of the ground plane resulting in changes in radiation patterns, especially the axial ratio performances. The simulation results show the ground plane size influences the antenna characteristics, especially the gain and axial ratio of the developed antenna.

The developed antenna is thinner, smaller, simpler and more compact compared to the previous antennas [6, 7]. In the next research, the developed antenna will be employed in an array configuration to generate a dual-band frequency as discussed in [6, 7].

## 6 Acknowledgments

The authors thank M. Takahashi for valuable opinions; T. Tanaka, K. Kaneko, and D. Ishide for the antenna fabrication and the measurements; the Japan Society for the Promotion of Science (JSPS) for the Grant-in-Aid for Scientific Research (Project no. 16360185); the National Institute of Information and Communications Technology – NICT (former Communication Research Laboratory – CRL), Japan for the joint research in ETS-VIII project; and the Centre for Frontier Electronics and Photonics – Chiba University, the Futaba Foundation and Chiba Bank for the Nanohana Competition 2004 Award and Research Grants.

## 7 References

- 1 Jang, J.H., Tanaka, M., and Hamamoto, N.: 'Portable and deployable antenna for ETS-VIII'. Proc. Interim Int. Symp. on Antenna and Propagation, Yokosuka, Japan, 2002, pp. 49–52
- 2 Ito, K., Daniel, J.-P., and Lenormand, J.-M.: 'A printed antenna composed of strip dipoles and slots generating circularly polarised conical patterns'. Proc. IEEE Antennas and Propagation Soc. Int. Symp., San Jose, USA, 1989, pp. 632–635
- 3 Delaune, D., Tanaka, T., Onishi, T., Sri Sumantyo, J.T., and Ito, K.: 'A simple satellite-tracking stacked patch array antenna for mobile communications experiments aiming at ETS-VIII applications', *IEE Proc., Microw. Antennas Propag.*, 2004, **151**, (2), pp. 173–179
- 4 Ishihara, H., Yamamoto, A., and Ogawa, K.: 'A simple model for calculating the radiation patterns of antennas mounted on a vehicle roof'. Proc. Interim Int. Symp. on Antennas and Propagation, Yokosuka, Japan, 2002, pp. 548–551
- 5 James, J.R. and Hall, P.S. (Eds.): 'Handbook of microstrip antennas' (IEE, London, 1989), pp. 235–249
- 6 Sri Sumantyo, J.T., and Ito, K.: 'Simple satellite-tracking triangular-patch array antenna for ETS-VIII applications'. IEICE Technical Report, AP2003-236, 2004, pp. 39–44
- 7 Sri Sumantyo, J.T., Ito, K., Delaune, D., Tanaka, T., and Yoshimura, H.: 'Simple satellite-tracking dual-band triangular-patch array antenna for ETS-VIII applications'. Proc. IEEE Antennas and Propagation Soc. Int. Symp., Monterey, USA, 2004, pp. 2500–2503
- 8 Balanis, C.A.: 'Antenna Theory' (Wiley, New York, 1997), Chap. 14, pp. 760–762
- 9 Teshirogi, T.: 'Basics and reality of antenna measurement methods', Textbook of IEICE-AP Workshop, (IEICE, Tokyo, 2005), p. 60 (in Japanese)
- 10 Sri Sumantyo, J.T., Ito, K., Delaune, D., Tanaka, T., Onishi, T., and Yoshimura, H.: 'Numerical analysis of ground plane size effects on patch array antenna characteristics for mobile satellite communications', *Int. J. Numer. Model.*, 2005, **18**, (2), pp. 95–106
- 11 Huang, J.: 'The finite ground plane effect on the microstrip antenna radiation patterns', *IEEE Trans. Antennas Propag.*, 1983, **31**, (4), pp. 649–653